Achieving Colossal Negative Thermal Expansion in Cubic Double ReO_3 Type Fluorides though Resonance-like Coupling of Phonon Vibration Modes

Dahu Chang(常大虎)[1, 2, 3], *Liying Zhang*(张丽莹)[2 *], *Xiaowei Huang*(黄晓伟)[2], *and Yu Jia*(贾瑜)[2, 3 *]

[1] Department of Mathematics and Physics, Luoyang Institute of Science and Technology, Luoyang 471023, China

[2] Key Laboratory for Special Functional Materials of Ministry of Education, and School of Materials Science and Engineering, Henan University, Kaifeng, 475001, China

[3] International Laboratory for Quantum Functional Materials of Henan, and School of Physics and Engineering, Zhengzhou University, Zhengzhou 450001, China

KEYWORDS: Colossal Negative Thermal Expansion; Coupling of Phonon Vibration Modes; First-principles Calculations and the Quasi-harmonic Approximation; Mode Grüneisen Parameters; Flexible Rocking Motion

---

* Corresponding authors: zhangly@henu.edu.cn; jiayu@henu.edu.cn

ABSTRACT: The design of materials with colossal negative thermal expansion (NTE) is of significant fundamental and technological importance in the field of thermal engineering. Using the first-principles calculations and the quasi-harmonic approximation (QHA), the NTE properties of cubic double ReO_3-type $M^{II}X^{IV}F_6$ (M=Mg, Ca, Sr, and X=Zr, Hf) are systematically investigated. We find that these fluorides exhibit relatively large NTE over a wide coefficient range, especially for $CaHfF_6$ and $SrHfF_6$ which the coefficients of NTE (CNTEs) can reach up to -70~75$\times 10^{-6}$ K^{-1}, being about two times more than that of ScF_3 with similar structure. By analyzing the changes of vibration frequency and negative Grüneisen parameters(NGP), we reveal that the underlying physics of such colossal NTE is attributed to the so-called resonance-like effect of two unique transverse vibration modes with nearly the same frequencies at both the Γ and X points in the Brillouin zone(BZ), which in turn greatly enhance the lattice distortion through flexible rotations of the MF_6 and XF_6 octahedrons. Our studies provide deep insights of the underlying mechanism of NTE in $M^{II}X^{IV}F_6$ fluorides, consequently offering a route for the design of colossal NTE materials.

PACS number(s): 65.40. De, 63.20.-e

1. Introduction

ScF_3, a typical ReO_3 structure consisted of ScF_6 octahedrons connecting by F atoms, processes the strong and isotropic NTE property over wide temperature ranges[1-7]. Compared with

complex oxides with NTE discovered previously [8-10], it provides a simple and ideal model for exploring the NTE mechanism of open-framework materials. During the passing decade both experimental and theoretical studies have identified that the NTE origins from the low frequency transverse vibration of F atom, and further called "guitar-string" effect[4]. However, the number of existing metallic fluorides with NTE property is very limited, instead, most metallic fluorides show positive thermal expansion(PTE) characteristics. Therefore, designing more fluorides with colossal NTE and widely temperature window on demand is not only the premise for the effective application of its NTE characteristics, but also a great challenge in this field. Fortunately, recent experiments reveal that the compensated co-substitution of Sc atoms in ScF_3 can form the double ReO_3units fluorine compounds $M^{II}X^{IV}F_6$ (M= Mg, Ca, Sr, Fe, Mn; X=Zr, Hf, Nb) or, $M^{I}X^{V}F_6$ (M= Li, Na; X=Sb), of which the thermal expansion properties can be tuned by choosing the appropriate metal cation, i.e., from large NTE to zero, to large PTE[6, 11-22].

In practice, $M^{II}X^{IV}F_6$ can adopt a rhombohedral ($R\bar{3}$) or a cubic ($Fm\bar{3}m$) phase, which are related to the differences of atomic radius and their corresponding electronegativity of M and X atoms[6, 11, 23]. For example, $LiSbF_6$-type usually refers to the rhombohedral structure and exhibit the PTE property because of the large difference of electronegativity between Li and Sb atoms[13]. Notwithstanding, for some of $M^{II}X^{IV}F_6$ compounds which maintain ideal cubic symmetry, the difference of both atomic radii and their electronegativity of M and X will certainly stabilize or destabilize the cubic structure and hence are likely to preclude less or strong NTE property than that of ScF_3[11-12]. Indeed, it has been discovered recently that $CaZrF_6$ displays a very large and isotropic NTE property (α_v ~ $^{-6}K^{-1}$ at 100 K),[11] even greater than the current most popular NTE materials like ZrW_2O_8 or ScF_3. With the replacement of Nb and Hf for Zr, further experiment shown that the CNTEs are even larger (α_v ~ $^{-6}K^{-1}$) both for $CaNbF_6$ and

$CaHfF_6$ at low temperature[16]. Also, it is interesting to note that the temperature window of NTE of $CaZrF_6$ can range from below 10 K to 1173 K or even higher[11], thus making this material the largest one at present.

Naturally, why does the thermal expansion of $M^{II}X^{IV}F_6$ behave remarkably differently? To address this issue, Hancock *et al.* first prepared the $CaZrF_6$ compound and pointed out that the most negative Grüneisen parameters(NGPs) that contribute to the NTE are associated with phonon modes below ~4.5 THz[11] . Sanson *et al.* further addressed that the dominant mode is the F_{1g} mode, located at 1.23 THz with the NGP of −34.9 at the Γ-point[24]. Using the first-principles calculations, Gupta *et al.* studied the NTE behavior in $MZrF_6$ (M = Ca, Mg, Sr), and they show that the NTE behavior positively relates to the anisotropy in the thermal amplitude of the fluorine atoms[17]. Xing *et al.* systematically designed a series of $MZrF_6$ (M = Ca, Mn, Fe, Co, Ni, and Zn) and realized the controllable isotropic thermal expansions from NTE to PTE effectively[12]. They also proposed two phenomenological rocking models to explain the various mechanism of thermal expansion properties. In all, in a sense the existing studies only qualitatively explain why the NTE property of these materials are different, but it is still impossible to answer why some $M^{II}X^{IV}F_6$ have the unexpected colossal coefficients of NTE, especially, they can be two or three times larger than ScF_3. From this point of view, it is very necessary to quantitatively understand the physical origins for the great difference of CNTE, and then find the novel NTE mechanism [11-12, 24].

In this work, we systematically investigate the NTE behavior of $M^{II}X^{IV}F_6$ (M = Mg, Ca, Sr; X=Zr, Hf) and explore the underlying mechanisms by employing first-principles calculations combined with the quasi-harmonic approximation (QHA). We found that the CNTEs of $M^{II}X^{IV}F_6$ increase with increasing the atomic numbers of both M and X[11]. The analysis of both

vibration modes and NGP reveal that the NTE behavior of $M^{II}X^{IV}F_6$ mainly originates from the synergetic effect of two transverse vibration modes at Γ and X points of Brillouin zone (BZ), which have nearly the same frequencies and the same large NGPs. A resonance-like model was proposed, with which we can well explain the difference of CNTE of these compounds quantitatively. Based on our findings, we also explain the recent experimental results that the CNTE can be effectively tuned by inserting small He atoms into $CaZrF_6$.

2. Results and discussion

Our density-functional theory (DFT) calculations have been performed using the Vienna *ab initio* simulation package with a plane-wave basis set[25], and the details of calculation are given in the Supplementary Materials (SM). $CaZrF_6$ or $CaHfF_6$ have been confirmed to have cubic structure with the space group Fm-3m, which contains Z = 4 formula units in the conventional unit cell [see Fig. 1(a)]. Alternately ordered CaF_6 (or MgF_6) and ZrF_6 (or HfF_6) octahedrons are connected by sharing F atoms in three dimensionally array, while the Ca^{2+} and Zr^{4+} (or Hf^{4+}) cations exhibit a NaCl-type packing. This ordered double ReO_3-type fluorides have the same structures as ABO_3 perovskites, but leave the A-cation sites vacant [see Fig. 1(c)]. Such an absence of octahedron units in the A-cation sites indeed allows MF_6 and XF_6 octahedrons to induce a flexible rotation. The optimized lattice constants of cubic $MgZrF_6$, $CaZrF_6$, and $CaHfF_6$, together with the bulk modulus of $CaZrF_6$, are in good agreement with both experimental and theoretical data[see Table S1[11-12, 24]]. The calculated bulk moduli of $M^{II}X^{IV}F_6$ family are all relative small that could be classified as soft materials, which can easily render a NTE behavior [26].

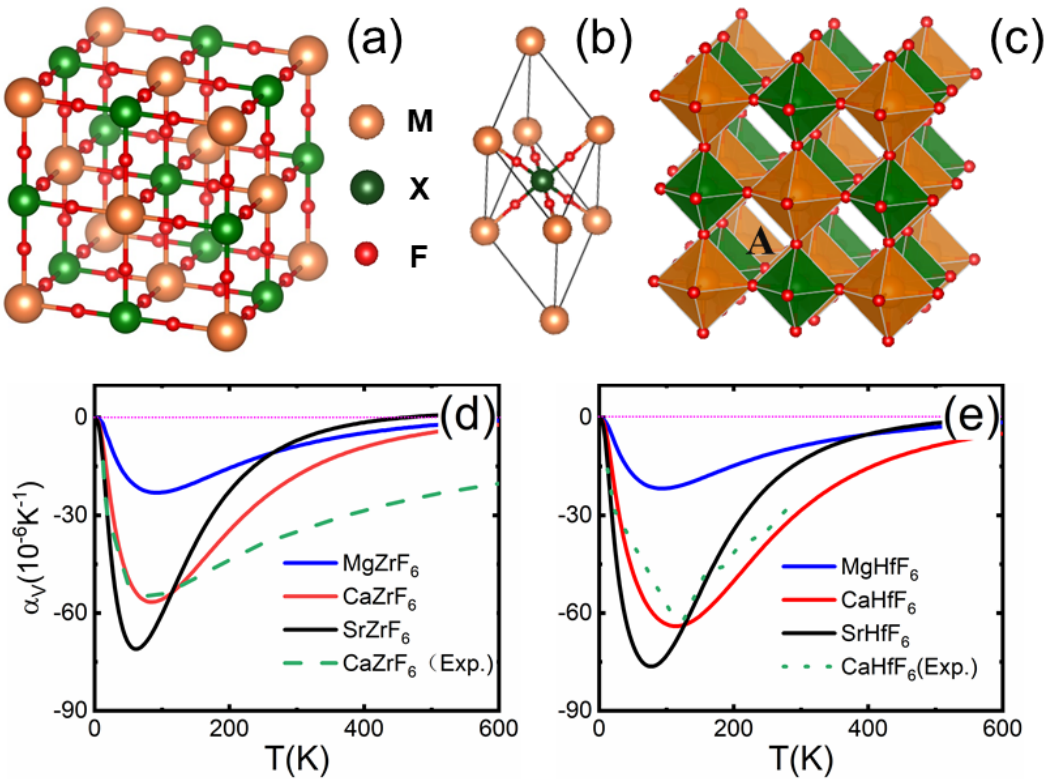


FIG. 1. Geometric structures and coefficients of negative thermal expansion α_V of $M^{II}X^{IV}F_6$ family. Schematic diagram of geometric structure in (a) conventional unit cell with double ReO_3-type grid units connected by F atoms, (b) primitive unit cell, respectively. (c) the corresponding Brillouin zone (BZ). The bulk coefficients α_V of negative thermal expansion in (d) $MZrF_6$(M=Mg, Ca, and Sr), and (e) $MHfF_6$(M=Mg, Ca, and Sr), respectively. The pink dashed line is a guide for the zero coefficient of thermal expansion. The green dashed line in (d) and (e) are from experimental data[11].

To explore the NTE properties of $M^{II}X^{IV}F_6$ (M = Mg, Ca, Sr; X = Zr, Hf) family, we calculate their phonon dispersion curves along the high symmetry lines in BZ. Considering that the influence of LO/TO splitting is mainly reflected in the high-frequency vibration modes, and the vibration modes that contributes to NTE come from the low-frequency parts[11, 17, 24] (see Fig. S1

in the SM for ScF_3 as an example), we present the results of phonon dispersion curves without the LO/TO splitting in our following discussion. The phonon dispersion curves, alongside with their corresponding phonon partial density of states (DOS) are shown in Fig.S2 (a)-(f). The low frequency vibration modes of M and X atoms have the following features: (i) the peak of the vibration modes originating from M atoms decreases from high frequency for Mg to low frequency for Sr, suggesting that its driven vibration frequency decreases monotonously as increasing the atomic number of M alkali element. (ii) The vibration modes originating from X atoms are nearly unchanged, but the magnitude of their lowest partial DOS increases from Zr to Hf (See the red peaks around 70 cm^{-1} in Fig. S2). This implies that the vibration modes originating from X atoms are more populated in lower-frequency range as the atomic number of X atom increases. Based on the above two features of the atomic-resolved vibration modes, it is most likely that the possible NTE properties of $M^{II}X^{IV}F_6$ family would become more pronounced with increasing the atomic number of either M atom in group IIA or X atom in group IVB. Similar to ScF_3, the common feature of $M^{II}X^{IV}F_6$ is that the lowest transverse optical phonon mode overlaps the lowest acoustic one around the BZ center (see Fig. S2). There exists a flat phonon band along Γ-X with unchanged frequency. Especially, the vibration frequency of the lowest transverse optical phonon mode at the X point is even lower than that of the lowest acoustic ones (see the black arrows in Fig. S2, and Table S1)[11-12], as discussed latter on.

Fig. 1 (d) and (e) are the CNTEs of $M^{II}X^{IV}F_6$ (M = Mg, Ca, Sr; X = Zr, Hf) family as a function of temperature. It is found that $CaZrF_6$ exhibits NTE properties in the temperature range between 0 ~850 K, with the CNTE of $-57\times10^{-6}K^{-1}$ at 85 K. This is consistent with experimental data that NTE temperature window is 0 ~ 1000 K and the largest CNTE of $-54\times10^{-6}K^{-1}$ [11]. Also, the largest CNTE for $CaHfF_6$ is found to be $-65\times10^{-6}K^{-1}$ at 110 K, which again agrees well with

the experimental value of $-66\times10^{-6}K^{-1}$ [11]. We notice that although the anharmonic effects in the interatomic potential become conspicuous in determining the thermal expansion property at high temperatures and the evaluation of the CNTE within the QHA would deviate from the experimental data at high temperatures, anyway, above results show that our calculation scheme is reasonable and can reflect its physical essential characteristics. In particular, we find that replacing Ca with Sr induces an enhancement from $-64\times10^{-6}K^{-1}$ to nearly $-78\times10^{-6}K^{-1}$ for $SrHfF_6$ compound. In contrast, the change in CNTE is much more pronounced when replacing Ca with Mg, which is only one third of its parentage (~ $^{-6}K^{-1}$) with the same geometry structures. Exploring the reasons behind such big differences would be useful for understanding the new NTE mechanism for $M^{II}X^{IV}F_6$ metal fluorides.

To explore the underlying mechanism of such big differences of NTE properties, as an example, we calculate the mode Grüneisen parameters (γ_i) as a function of frequency of $CaZrF_6$ and $CaHfF_6$, which is an indicator of NTE from the lattice vibration[27]. In Fig. 2(a) and (b), We find that the modes with low vibration frequencies (below ~200cm^{-1}) have significantly larger NGPs, and, in particular, there is a largest peak of NGP at a vibration frequency of ~ 25 cm^{-1}, which indicating that these vibration modes contributes to the NTE mostly[11].

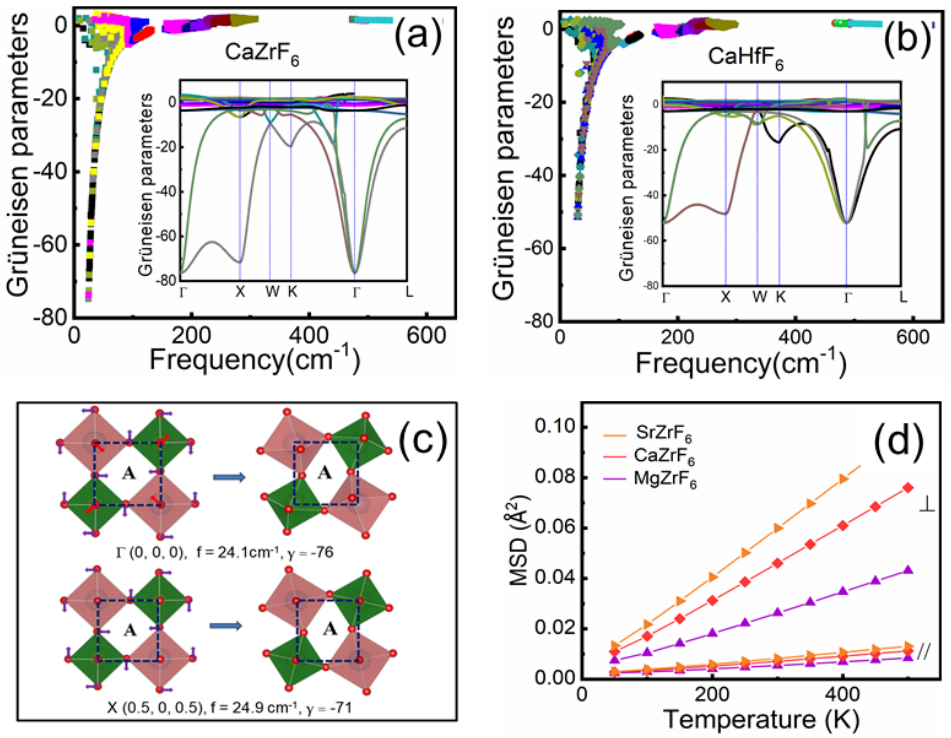


FIG. 2. The calculated mode Grüneisen parameters as a function of frequency in (a) $CaZrF_6$ and (b) $CaHfF_6$, respectively. The mode Grüneisen parameters via the high symmetry lines in BZ are also given as the insets respectively. (c) Schematic diagrams of the transverse vibration modes of $CaZrF_6$ at Γ (0, 0, 0) and X (0.5, 0, 0.5) points, respectively. The resulting positions of F atoms after displacement are also drawn. The red ball represents the F atom, and the pinky (green) octahedron represents the CaF_6 (ZrF_6) unit. (d) the mean square displacement of the longitudinal and transverse vibration of F atoms in $MgZrF_6$, $CaZrF_6$, and $SrZrF_6$, respectively.

To identify the vibration modes that have the greatest contribution to NTE, we calculated the Grüneisen parameters of vibration modes along the high symmetry lines in BZ for $CaZrF_6$ and $CaHfF_6$, as shown in the inset of Fig. 2(a) and (b), respectively. We find that the largest NGP at a vibration frequency of ~ 25 cm^{-1} corresponds to the lowest optical modes at Γ and X points (as well as Γ-X line). Like ScF_3, Fig. 2(c) and (d) shows the schematic diagrams for the lowest

optical vibration modes in $CaZrF_6$ at both Γ and X points. The mode of 24.1 cm^{-1} at Γ point corresponds to a transverse vibration of all F atoms, which is perpendicular to the directions of the Zr-F-Ca linkages. Meanwhile the mode of 24.9 cm^{-1} at the X point is almost the same transverse vibration of F atoms as that at the Γ point (as well as the Γ-X line), without the participation of the out-of-plane F atoms in the rotation of octahedron. The two transverse vibration modes of F atoms at the Γ and X points reduce the distance between the Zr and Ca atoms, and, in turn, the volume around the A-voids decreases, leading to a larger NTE (see Fig. 2(c)). We notice that in our calculations the CNTE increases with increasing the atomic radius of either M or X atoms in $M^{II}X^{IV}F_6$ family. As the atomic radius of both M and X increase, the distance between MF_6 and XF_6 octahedrons will increases, leading to an increase in NTE naturally[28]. However, considering the influence of different lattice constants on the CNTE, it is easy to estimate that the difference between the $CaZrF_6$ and $MgZrF_6$ is only about 20%, suggesting the displacement of F atom away from equilibrium positions are approximately proportional to the lattice constants. Clearly, it can't understand the results of the above theoretical calculations and experimental measurement.

In terms of real space, the motion of the F atom in $M^{II}X^{IV}F_6$ away from the equilibrium position is corresponding to a lot of vibrations modes with different wave vectors in reciprocal space, including low-frequency and high-frequency parts, and these wave vectors can be obtained by Fourier transform mathematically. In Fig. 2(d), we give the mean square displacement (MSD) of the motions of the F atom in the above compounds respectively. Again, it can be seen that the transverse MSD of $CaZrF_6$ and $SrZrF_6$ is more than twice than that of $MgZrF_6$, while the longitudinal MSD almost the same, indicating that the NTE is mainly determined by the

superposition of the two transverse vibration modes (of Γ and X points) with the largest NGPs[4, 17].

Now, we come to address the reasons behind the large difference in CNET when Ca is replaced by Mg in $M^{II}X^{IV}F_6$. First, we have sorted out the frequencies of the lowest optical vibration modes at both Γ and X points from Table S2, which correspond to the main contribution to NTE. And these results are replotted in Fig. 3(a) and (b), respectively. It is clear that there is almost no difference between the frequencies obtained at the Γ and X points both for $CaXF_6$ and $SrXF_6$, which implies that these two vibration modes (corresponding to the same transverse vibration of F atom in real space) can meet one of conditions of resonance of MF_6 and XF_6 octahedrons. Second, we also plotted the NGPs of above vibration modes at both Γ and X points, as shown in Fig. 3 (c) and (d). The NGPs of these two points are almost the same both for $CaXF_6$ and $SrXF_6$. **Given that relationship formula between the coefficient of negative thermal expansion and the Grüneisen parameter, $\alpha_V = \frac{C_V \bar{\gamma}}{BV}$, which the coefficient of negative thermal expansion α_V is directly proportional to the Grüneisen parameter $\bar{\gamma}$, and the magnitude of the negative Grüneisen parameter quantitatively reflects the equivalent contribution weight of this soft mode to the volume contraction effect, here we take the NGPs as "quasi-amplitude" of vibration.**[29]. Combining the above two factors and taking the NGPs as "quasi-amplitude" of vibration, we can conclude that the two vibration modes in $M^{II}X^{IV}F_6$ (M= Ca, Sr; X=Zr, Hf) can be perfectly coupled to form a resonance-like effect. We have noted that the vibrations between $\Gamma - X$ line in BZ have the same frequencies (correspond to the transverse vibration of F atom) with NGPs, which greatly increases the CNTE via such resonance-like effect. But for $MgXF_6$, as shown in Fig.3(c)-(d), the differences of both the vibration frequency and the NGP between Γ

and X points are obvious and there should no such resonance-like effect occurred. Thus, the CNTEs of $MgXF_6$ are much smaller although they have the relatively large NGP at Γ point. In our calculations, the CNTE of $MgZrF_6$ is only ~ $^{-6}K^{-1}$, just about one third of $CaZrF_6$.

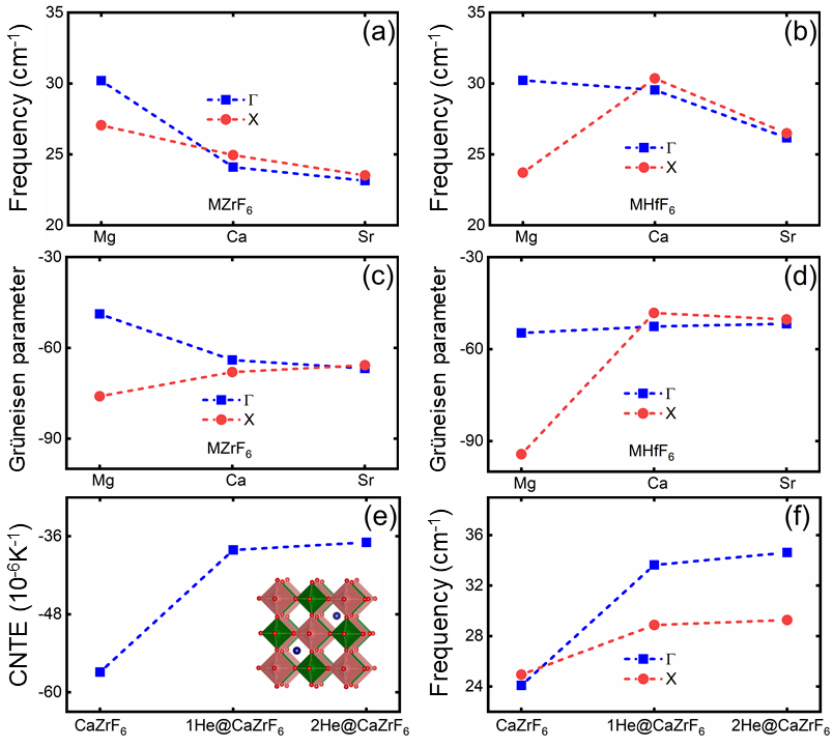


FIG. 3. The lowest optical vibration frequency of NTE modes for (a) $MZrF_6$ (M=Mg, Zr, Sr), (b) $MHfF_6$ (M=Mg, Zr, Sr) taken at the Γ and X points in BZ; The NGP of the lowest optical vibration mode for (c) $MZrF_6$ (M=Mg, Zr, Sr), (d) $MHfF_6$ (M=Mg, Zr, Sr) taken at the Γ and X points in BZ. (e) the CNTE for $CaZrF_6$, 1He @ $CaZrF_6$ and 2He @ $CaZrF_6$, respectively. The inset shows the structure of 2He @ $CaZrF_6$. (f) the calculated frequency of the lowest energy optical modes at Γand X points for each system above.

Since $CaZrF_6$ with double ReO_3-type units can be considered to be obtained by compensated co-substitution in ScF_3 structure, it is of interest whether this kind of resonance-like effect will exist

in ScF_3. To this end, we calculated the NTE property of ScF_3 with double rigid units by employing an enlarged $2\times2\times2$ supercell. It is surprising that the vibration frequencies are obvious difference, being ~19 cm^{-1} at Γ point and ~23 cm^{-1} at X point. In terms of frequency of vibration mode, we see that the frequency of low-frequency vibration modes of ScF_3 are lower than that of $CaZrF_6$, and it indicates that ScF_3 should have a larger CNTE than that of $CaZrF_6$. Unfortunately, the CNTE of ScF_3 is only one half or one third of that of $M^{II}X^{IV}F_6$ (M= Ca, Sr; X=Zr, Hf), owning to no obvious resonance-like effect in it. In short, the CNTE of open-frame structures depends not only on whether its vibration modes have large NGPs, but also on the effective coupling between its vibration modes. In other words, even if the vibration modes have the large NGPs, if these vibration modes are out of phase, the material will not have a large NTE characteristic. In that sense, our finding provides a solution for designing colossal NTE materials.

Here we give a simple analysis of such resonance-like effect, we assume that the F atoms A, B, C, and D at the four vertices of the *xy* plane in the voids surrounded by SrF_6 and HfF_6 octahedra vibrate inward and outward in different modes, respectively. According to our previous analysis (see Fig.2(c) and Fig.4), A and B correspond to the lateral horizontal vibration of two atoms, with a frequency of ω_1 and an amplitude of $dx=\Delta x\cos(\omega_1 t+\varphi_1)$. While C and D correspond to longitudinal vertical vibrations with a frequency of ω_2 and an amplitude of $dy=\Delta y\cos(\omega_2 t+\varphi_2)$. The average variation of the area ΔS in the Fig.4 can be given by the following equation,

$$\Delta S=S_0-\frac{2}{T_2T_1}\int_0^{T_1T_2}(x_0-\Delta x\cos(\omega_1 t+\varphi_1)(y_0+\Delta y\cos(\omega_2 t+\varphi_2)dt$$

Here, x_0, y_0, and S_0 correspond to the length of the edges and the area of the voids of the polyhedron at the equilibrium position, respectively. Δx and Δy are the maximum

displacements away from the equilibrium positions, and we take $\Delta x = \Delta y = 0.05$ Å, as shown in Fig.2 (d) in the manuscript. The result is show in Fig.4, it can be seen that if the frequencies of the two vibration modes are the same, the change in voids contraction will be significant. Similarly, these conclusions also apply to the *xz* and *yz* planes. Of course, at the same frequency, the volume contraction caused by this resonance-like modes will be greater. In other words, they exhibit the larger coefficient of negative thermal expansion. Our numerical simulation shows that result remains unchanged as long as the difference of phases is constant.

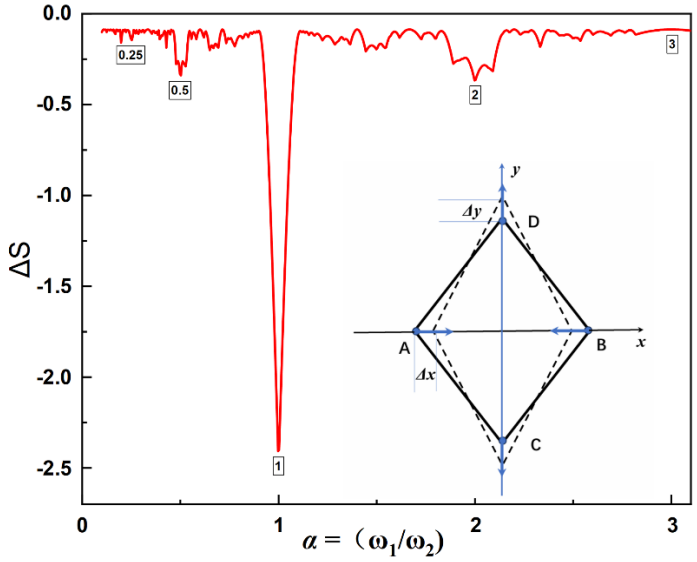


FIG. 4. Simulation results of coupling two negative expansion vibration modes with different frequencies, when the frequency is the same, negative expansion is significant.

Furthermore, we show that such resonance-like effect in $CaZrF_6$ can be tuned by inserting the small inert gas molecules on the A sites (e.g., He atom). Experimentally, Hester *et al.* have shown that the CNTE is reduced dramatically by inserting He atom in $CaZrF_6$[30]. To explain the experimental results based on the resonance-like model, we have calculated CNTE of $CaZrF_6$, as well as the vibration frequency of Γ and X point in BZ, by inserting one (1He@$CaZrF_6$) and two

He atoms (2He@$CaZrF_6$), and the results are shown in Fig. 3(e) and (f) respectively. It is found that the CNTE of 1He@$CaZrF_6$ reduces to ~ $^{-6}K^{-1}$ (~ $^{-6}K^{-1}$ in 2He@$CaZrF_6$), which is only one half of that of pure $CaZrF_6$. The reasons responsible for the change of CNTE of 1He@$CaZrF_6$ are two-fold. One is that the difference of vibration frequency at Γ and X point of BZ becomes obvious (see Fig. 3(f)) and the resonance-like effect is therefore disappeared. Another is associated with the increasing frequency of the lowest optical vibration modes at Γ and X point in BZ. This again confirms that the proposed resonance-like modes are credible and it will play a key role in tuning the magnitude of NTE properties in materials.

3. Conclusions

In summary, based on first-principles density functional theory calculations in combination with the QHA, we have investigated the NTE properties of double ReO_3-type $M^{II}X^{IV}F_6$ family. We find that they exhibit a significantly enhanced NTE behavior, which the CNTE can reach up to $-60 \sim$ $^{-6}K^{-1}$. By the analyses of the frequencies and NGPs of vibration modes, a simple picture in terms of the flexible rocking motion of MF_6 and XF_6 octahedrons has proposed, which CNTE can be effectively enhanced by resonance-like effect of the vibration modes in BZ. Our finding not only enrich our understanding of the underlying mechanism of NTE in open-fame structures, but also facilitate the future development and applications of these NTE metallic fluorides materials, as well as oxides.

Corresponding Author

* Corresponding authors: zhangly@henu.edu.cn; jiayu@henu.edu.cn

Conflicts of interest

There are no conflicts of interest to declare.

ACKNOWLEDGMENT

We thank Professor Zaiping Zeng in Henan University for helpful discussions and revise manuscript, and YJ thanks Martin Dove in Sichuan University for helpful discussions. This study was supported by the National Natural Science Foundation of China (Nos.11774078, 22090042, 12074099) and National Key R&D Program of China (2020YFA0406202) and Natural Science Foundation of Henan Province (Grant No.242300420257).

REFERENCES

[1] Li C W, Tang X, Muñoz J A, Keith J B, Tracy S J, Abernathy D L and Fultz B, 2011 *Phys. Rev. Lett.* **107** 195504

[2] Yang C, Tong P, Lin J, Guo X, Zhang K, Wang M, Wu Y, Lin S, Huang P and Xu W, 2016 *Appl. Phys. Lett.* **109** 023110

[3] Hu L, Qin F, Sanson A, Huang L-F, Pan Z, Li Q, Sun Q, Wang L, Guo F and Aydemir U, 2018 *J. Am. Chem. Soc.* **140** 4477

[4] Hu L, Chen J, Sanson A, Wu H, Guglieri Rodriguez C, Olivi L, Ren Y, Fan L, Deng J and Xing X, 2016 *J. Am. Chem. Soc.* **138** 8320

[5] Greve B K, Martin K L, Lee P L, Chupas P J, Chapman K W and Wilkinson A P, 2010 *J. Am. Chem. Soc.* **132** 15496

[6] Bird T, Woodland-Scott J, Hu L, Wharmby M, Chen J, Goodwin A and Senn M, 2020 *Phys. Rev. B* **101** 064306

[7] Cheng D, He Y, Liu S, Su N and Sun Y, 2025 *Chinese Physics B* **34** 067505

[8] Mary T A, Evans J S O, Vogt T and Sleight A W, 1996 *Science* **272** 90

[9] Hancock J, Turpen C, Schlesinger Z, Kowach G and Ramirez A, 2004 *Phys. Rev. Lett.* **93** 225501

[10] Gupta M, Mittal R and Chaplot S, 2013 *Phys. Rev. B* **88** 014303

[11] Hancock J C, Chapman K W, Halder G J, Morelock C R, Kaplan B S, Gallington L C, Bongiorno A, Han C, Zhou S and Wilkinson A P, 2015 *Chem. Mater.* **27** 3912

[12] Hu L, Chen J, Xu J, Wang N, Han F, Ren Y, Pan Z, Rong Y, Huang R, Deng J, Li L and Xing X, 2016 *J. Am. Chem. Soc.* **138** 14530

[13] Yang C, Qu B Y, Pan S S, Zhang L, Zhang R R, Tong P, Xiao R C, Lin J C, Guo X G, Zhang K, Tong H Y, Lu W J, Wu Y, Lin S, Song W H and Sun Y P, 2017 *Inorg. Chem.* **56** 4990

[14] Hester B R, Hancock J C, Lapidus S H and Wilkinson A P, 2017 *Chem. Mater.* **29** 823

[15] Xu J, Hu L, Song Y, Han F, Qiao Y, Deng J, Chen J and Xing X, 2017 *J. Am. Ceram. Soc.* **100** 5385

[16] Hester B R and Wilkinson A P, 2018 *Inorg. Chem.* **57** 11275

[17] Gupta M, Singh B, Mittal R and Chaplot S, 2018 *Phys. Rev. B* **98** 014301

[18] Wang N, Deng J, Chen J and Xing X, 2019 *Inorganic Chemistry Frontiers* **6** 1022

[19] Hester B R and Wilkinson A P, 2019 *J. Solid State Chem.* **269** 428

[20] Sanson A, 2019 *Materials Research Letters* **7** 412

[21] Qiao Y, Zhang S, Zhang P, Guo J, Sanson A, Zhen X, Zhao K, Gao Q and Chen J, 2024 *Nano Research* **17** 2195

[22] Zhao K, Jiao Y, Sun Q, He R, Sanson A, Zhong Z, Liang E and Gao Q, 2024 *Phys. Rev. B* **110** 064322

[23] Rodriguez V, Couzi M, Tressaud A, Grannec J, Chaminade J and Soubeyroux J, 1990 *J. Phys.: Condens. Matter* **2** 7373

[24] Sanson A, Giarola M, Mariotto G, Hu L, Chen J and Xing X, 2016 *Mater. Chem. Phys.* **180** 213

[25] Georg K and Jürgen F, 1996 *Phys. Rev. B* **54** 11169

[26] Fang H and Dove M T, 2013 *Phys. Rev. B* **87** 214109

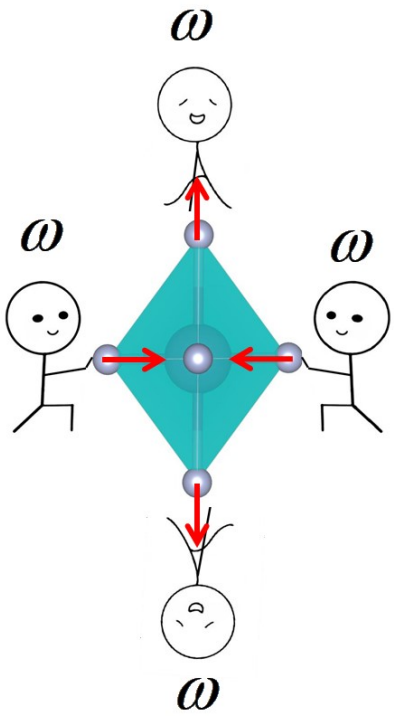
[27] Wang Z, Wang F, Wang L, Jia Y and Sun Q, 2013 *J. Appl. Phys.* **114** 063508

[28] Forster P, Yokochi A and Sleight A, 1998 *J. Solid State Chem.* **140** 157

[29] Ashcroft N W and Mermin N D, Solid State Physics. Saunders College Publishing: 1976.

[30] Hester B R, Dos Santos A M, Molaison J J, Hancock J C and Wilkinson A P, 2017 *J. Am. Chem. Soc.* **139** 13284

TOC



Negative thermal expansion is the result of the interaction between positive and negative expansion vibration modes.